NASA/TM—2007-214931

An Elongated Tetrakaidecahedron Model for Open-Celled Foams

Roy M. Sullivan
Glenn Research Center, Cleveland, Ohio

Louis J. Ghosn
Ohio Aerospace Institute, Brook Park, Ohio

Bradley A. Lerch
Glenn Research Center, Cleveland, Ohio

July 2007

NASA STI Program . . . in Profile

Since its founding, NASA has been dedicated to the advancement of aeronautics and space science. The NASA Scientific and Technical Information (STI) program plays a key part in helping NASA maintain this important role.

The NASA STI Program operates under the auspices of the Agency Chief Information Officer. It collects, organizes, provides for archiving, and disseminates NASA's STI. The NASA STI program provides access to the NASA Aeronautics and Space Database and its public interface, the NASA Technical Reports Server, thus providing one of the largest collections of aeronautical and space science STI in the world. Results are published in both non-NASA channels and by NASA in the NASA STI Report Series, which includes the following report types:

- TECHNICAL PUBLICATION. Reports of completed research or a major significant phase of research that present the results of NASA programs and include extensive data or theoretical analysis. Includes compilations of significant scientific and technical data and information deemed to be of continuing reference value. NASA counterpart of peer-reviewed formal professional papers but has less stringent limitations on manuscript length and extent of graphic presentations.

- TECHNICAL MEMORANDUM. Scientific and technical findings that are preliminary or of specialized interest, e.g., quick release reports, working papers, and bibliographies that contain minimal annotation. Does not contain extensive analysis.

- CONTRACTOR REPORT. Scientific and technical findings by NASA-sponsored contractors and grantees.

- CONFERENCE PUBLICATION. Collected papers from scientific and technical conferences, symposia, seminars, or other meetings sponsored or cosponsored by NASA.

- SPECIAL PUBLICATION. Scientific, technical, or historical information from NASA programs, projects, and missions, often concerned with subjects having substantial public interest.

- TECHNICAL TRANSLATION. English-language translations of foreign scientific and technical material pertinent to NASA's mission.

Specialized services also include creating custom thesauri, building customized databases, organizing and publishing research results.

For more information about the NASA STI program, see the following:

- Access the NASA STI program home page at *http://www.sti.nasa.gov*

- E-mail your question via the Internet to *help@sti.nasa.gov*

- Fax your question to the NASA STI Help Desk at 301–621–0134

- Telephone the NASA STI Help Desk at 301–621–0390

- Write to:
  NASA Center for AeroSpace Information (CASI)
  7115 Standard Drive
  Hanover, MD 21076–1320

NASA/TM—2007-214931

An Elongated Tetrakaidecahedron Model for Open-Celled Foams

Roy M. Sullivan
Glenn Research Center, Cleveland, Ohio

Louis J. Ghosn
Ohio Aerospace Institute, Brook Park, Ohio

Bradley A. Lerch
Glenn Research Center, Cleveland, Ohio

National Aeronautics and
Space Administration

Glenn Research Center
Cleveland, Ohio 44135

July 2007

Acknowledgments

The authors are grateful for funding from the External Tank Project under NASA's Space Shuttle Program.

Level of Review: This material has been technically reviewed by technical management.

Available from

NASA Center for Aerospace Information
7115 Standard Drive
Hanover, MD 21076–1320

National Technical Information Service
5285 Port Royal Road
Springfield, VA 22161

Available electronically at http://gltrs.grc.nasa.gov

An Elongated Tetrakaidecahedron Model for Open-Celled Foams

Roy M. Sullivan
National Aeronautics and Space Administration
Glenn Research Center
Cleveland, Ohio 44135

Louis J. Ghosn
Ohio Aerospace Institute
Brook Park, Ohio 44142

Bradley A. Lerch
National Aeronautics and Space Administration
Glenn Research Center
Cleveland, Ohio 44135

Abstract

A micro-mechanics model for non-isotropic, open-celled foams is developed using an elongated tetrakaidecahedron (Kelvin model) as the repeating unit cell. The micro-mechanics model employs an elongated Kelvin model geometry which is more general than that employed by previous authors. Assuming the cell edges possess axial and bending rigidity, the mechanics of deformation of the elongated tetrakaidecahedron lead to a set of equations for the Young's modulus, Poisson's ratio and strength of the foam in the principal material directions. These equations are written as a function of the cell edge lengths and cross-section properties, the inclination angle and the strength and stiffness of the solid material. The model is applied to predict the strength and stiffness of several polymeric foams. Good agreement is observed between the model results and the experimental measurements.

1. Introduction

Previous studies on open and closed-cell foams have sought to establish a direct tie between the foam microstructure and the macro-level foam properties. Through careful consideration of the foam micro-structure and selection of a suitable representative repeating unit, equations for the foam density, elastic constants and strength have been written in terms of the micro-structural dimensions and the physical and mechanical properties of the solid material (Gent and Thomas (1959), Dement'ev and Tarakanov (1970), and Huber and Gibson (1988)).

To represent the foam micro-structure, many of these previous researchers used a tetrakaidecahedron, a fourteen-sided polyhedron comprised of six quadrilateral and eight hexagonal faces. The tetrakaidecahedron is widely known as the Kelvin foam model, as it was Thomson (1887) who, in his assessment of Plateau's experiment, identified the tetrakaidecahedron (with slightly curved faces) as the only polyhedron that packs to fill space and minimize the surface area per unit volume (Gibson and Ashby (1997)). Zhu, et al. (1997), for example, adopted an equi-axed tetrakaidecahedron to develop equations for the foam Young's modulus, shear modulus and Poisson's ratio for isotropic, open-celled foams. They assumed that the mechanical behavior of open-celled foams could be simulated by treating the edges of the cell faces as structural elements possessing axial, bending and torsional rigidity. Applying the principle of minimum potential energy to the deformation of the repeating unit, the equations for the foam elastic constants were written in terms of the cell edge length L, the edge cross-sectional area A, moment of inertia I and polar moment of inertia J and the Young's modulus E and shear modulus G of the solid material. Using a similar set of assumptions, Warren and Kraynik (1997) developed similar equations for the Young's modulus, bulk modulus and shear modulus for isotropic,

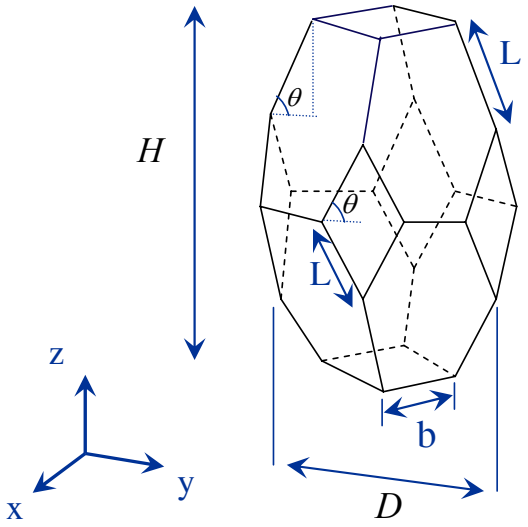

Figure 1.—Elongated tetrakaidecahedron repeating unit cell.

open-celled foams. The more recent model by Gong, et al. (2005a) includes the effect of shear deformation and allows for the edge cross-sectional area to vary along the length of the edge.

In many cases, the foam micro-structure is elongated in one of the three orthogonal directions causing the foam mechanical behavior to be non-isotropic. The micro-structure in closed-cell foams, for example, is often elongated in the *rise* direction due to the foaming and rising process. To treat non-isotropic foams, Dement'ev and Tarakanov (1970), Gong, et al. (2005a, b), Ridha, et al. (2006) and others have adopted an elongated tetrakaidecahedron (fig. 1) as the repeating unit cell, deriving equations for the elastic constants and strengths in the principal material directions. An elongated tetrakaidecahedron also packs to fill the space. It contains eight hexagonal faces, two horizontal square faces and four vertical diamond faces. The horizontal square faces have sides of length b and the diamond faces have sides of length L. The hexagonal faces have four sides with length L and two sides with length b. The inclination angle θ defines the orientation of the hexagonal faces with respect to the rise direction as well as the obtuse angle of the vertical diamond faces.

The size and shape of the elongated tetrakaidecahedron is uniquely defined by specifying the value of the three dimensions: b, L and θ. The above mentioned authors, however, have developed their equations for the elastic constants and compressive strengths of non-isotropic foams by imposing the restriction on the cell geometry that $\frac{b}{L}=\sqrt{2}\cos\theta$. This constraint forces the cell shape to be a function of the inclination angle only. Since, from a purely geometrical point of view, θ and $\frac{b}{L}$ may vary independently, we see no reason for this restriction on the cell geometry, other than to reduce the number of micro-structural measurements required to apply the equations and predict the foam behavior. As such, it is prudent to revisit the formulation of the previous authors and re-derive the equations for the elastic constants and strengths using the most general description of the elongated Kelvin model geometry.

In this paper, we derive the equations for the Young's modulus, Poisson's ratio and strength for non-isotropic foams in the principal material directions. We follow closely the formulation from Zhu, et al. (1997), but adopt, as our repeating unit, an elongated Kelvin model with a geometry defined by three independent dimensions. Furthermore, we allow the edge cross-sections to assume any shape, but restrict our attention to edge cross-sections that do not vary along the edge length. In the application section, we make the simplifying approximation that the edge cross-sections are circular and apply the model to simulate the mechanical and strength behavior of several polymeric foams. In the final section, we extend the use of the model to closed-cell foams and predict the strength ratio of the five rigid polyurethane closed-cell foams studied by Huber and Gibson (1988).

2. Elongated Tetrakaidecahedron (Kelvin) Model

2.1 Cell Aspect Ratio

The size and shape of an elongated tetrakaidecahedron are uniquely defined by specifying the value of any three of the five dimensions L, b, θ, H, D, since the height H and width D of the unit cell is related to L, b, and θ according to

$$H = 4L\sin\theta \qquad \text{and} \qquad D = 2L\cos\theta + \sqrt{2}\,b \tag{1}$$

The cell aspect ratio $R = \frac{H}{D}$ is therefore

$$R = \frac{4L\sin\theta}{2L\cos\theta + \sqrt{2}\,b} \tag{2}$$

There is a minimum value of θ, below which the unit cell in figure 1 is no longer elongated in the Z-direction. This minimum value of θ is a function of the length ratio $\frac{b}{L}$, since as $\frac{b}{L}$ becomes larger, the value of θ must become larger in order for $H > D$ and thus $R > 1$. The equation for the minimum θ in terms of the ratio $\frac{b}{L}$ is derived in the Appendix.

2.2 Foam Relative Density

The relative density γ is, by definition, the ratio of the foam density to the density of the solid material, $\gamma = \frac{\rho}{\rho_s}$. The relative density may be written in terms of volumes as $\gamma = \frac{V_s}{V}$, where V_s is the volume occupied by solid matter and V is the total volume of the foam. Using the elongated tetrakaidecahedron shown in figure 1 as a representative volume, the total volume is $V = H D^2$. The members that form the perimeter of the vertical diamond faces and those of length b that form the perimeter of the horizontal square faces are shared by the adjacent cells. Thus, they contribute only half their cross-sectional area to the repeating unit. All other members are completely contained within the boundaries of the unit cell. The volume of solid material is therefore $V_s = 16AL + 8Ab$, where, again, A is the edge cross-sectional area. Using the relations in equation (1), the relative density may be written

$$\gamma = \frac{2A(2L + b)}{L\sin\theta\left[2L\cos\theta + \sqrt{2}b\right]^2} \tag{3}$$

2.3 Loading in the Y-direction (Perpendicular-to-Rise)

We now seek to develop equations for the foam mechanical response and foam strength, for loading in the y (perpendicular-to-rise) direction, in terms of the micro-structural dimensions L, b, and θ, the edge cross-section area A and moment of inertia I and the modulus E and ultimate strength σ^{ult} of the solid material. For this purpose, we establish the cartesian coordinate system shown in figure 2, where the

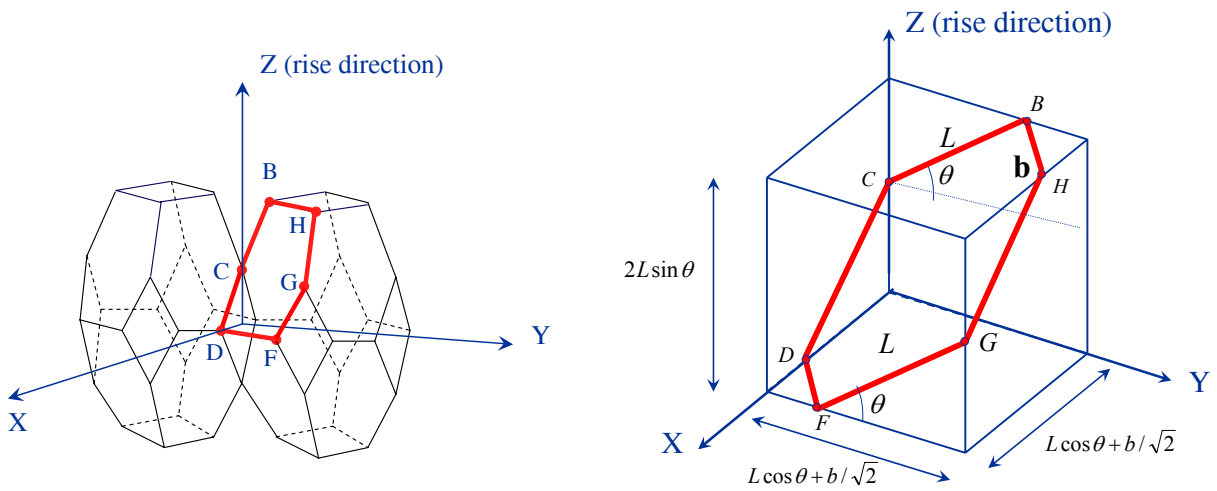

Figure 2.—Repeating unit cell for loading in the Y-direction (perpendicular to rise).

Z-direction is oriented in the rise direction and the X and Y directions are in the plane perpendicular to the rise direction. We will develop the equations for the foam mechanical response and strength for loading in the Y-direction and note that due to symmetry of the repeating unit cell, the same set of equations will apply for loading in the X-direction. Furthermore, due to symmetry, we can use the unit cell shown in figure 2, which represents one-eighth of the tetrakaidecahedron shown in figure 1.

We consider the deformation of this unit cell under the application of a uni-axial stress in the Y-direction σ_{yy} which results in an extension in the Y-direction and the accompanying contractions in the X- and Z-directions. In order for the unit cell to be a representative repeating unit during deformation, we enforce the symmetry conditions on the member end point displacements:

$$\begin{aligned} u_B &= u_C = 0 & \qquad u_F &= u_G = -\bar{u} \\ v_C &= v_D = 0 & \qquad v_G &= v_H = \bar{v} \\ w_D &= w_F = 0 & \qquad w_B &= w_H = -\bar{w} \end{aligned} \tag{4}$$

where u, v, and w denote the displacements in the X-, Y-, and Z-directions, respectively, and $\bar{u}$, $\bar{v}$, and $\bar{w}$ represent the displacements of the unit cell at the unit cell boundaries. We also require that the deformation of the unit cell occurs with no rotation of the member end points. In addition, we note that due to similarity of members *BC* and *FG* and the similarity of members *BH* and *DF*, we have the additional conditions

$$\begin{aligned} u_H &= u_F \\ v_H^B &= v_F \\ w_G &= w_B \end{aligned}$$

where v_H^B is the Y-direction relative displacement of point *H* with respect to point *B*, $v_H = v_B + v_H^B$.

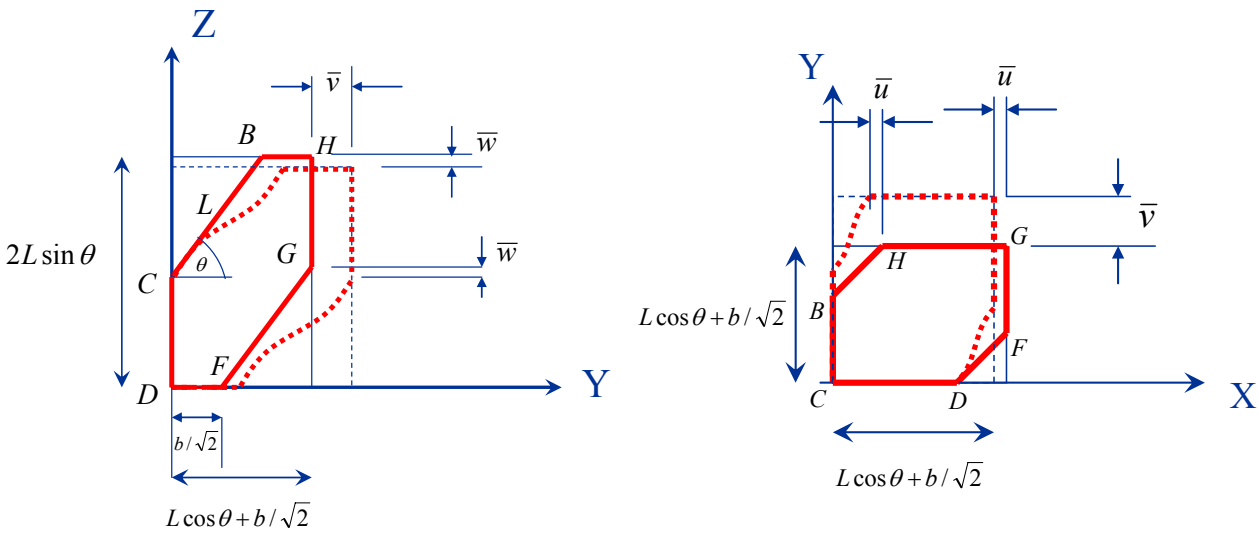

(a) Y-Z plane (b) X-Y plane

Figure 3.—Unit cell deformation for loading in the Y-direction.

The deformation of the unit cell is illustrated in figure 3. It is straightforward to write the strains in terms of the unit cell boundary displacements

$$\varepsilon_{xx}=\frac{-2\bar{u}}{2L\cos\theta+\sqrt{2}b} \qquad \varepsilon_{yy}=\frac{2\bar{v}}{2L\cos\theta+\sqrt{2}b} \qquad \varepsilon_{zz}=\frac{-\bar{w}}{2L\sin\theta} \tag{5}$$

Due to the loading on the unit cell and the restrictions on the displacements, the members *CD* and *GH* carry no axial load or bending moment and therefore they do not contribute to the strain energy. Furthermore, since the members *BC* and *FG* have the same length, orientation and stiffness and since the same is true for members *BH* and *DF*, the strain energy of the assemblage of members *BC* and *BH* are exactly equal to the strain energy of the assemblage of members *DF* and *FG*. Thus, the total strain energy of the deformation of the unit cell is

$$U=2\left(U_{BC}+U_{BH}\right) \tag{6}$$

and we need only consider further the deformation of members *BC* and *BH*.

Now since $v_H=\bar{v}$, we also have that $\left(\frac{v_B}{\bar{v}}\right)+\left(\frac{v_H^B}{\bar{v}}\right)=1$. Furthermore, it can be shown that, due to the relative stiffness of members *BC* and *BH*, the fractional displacements are

$$\frac{v_B}{\bar{v}}=\frac{2L\left(12I\cos^2\theta+AL^2\sin^2\theta\right)}{12I\left(2L\cos^2\theta+b\right)+A\left(2L^3\sin^2\theta+b^3\right)}$$

$$\frac{v_H^B}{\bar{v}}=\frac{b\left(12I+Ab^2\right)}{12I\left(2L\cos^2\theta+b\right)+A\left(2L^3\sin^2\theta+b^3\right)} \tag{7}$$

The strain energy for a single structural member carrying an axial force and bending moment is (Laible (1985))

$$U = \frac{N^2 L}{2AE} + \frac{1}{2EI}\int_0^L M^2(s)ds \tag{8}$$

where N is the axial force and $M(s)$ is the equation for the bending moment written as a function of the local length coordinate s, where s is oriented along the member length. We note that all members in the one-eighth unit cell have a cross-sectional area of $A/2$, since they are on the boundary of the unit cell and are shared by two adjacent unit cells. Likewise, the moment of inertia of members BC and BH is $I/2$, since, given the deformation of the unit cell specified by equation (4) and illustrated in figure 3, the axis of bending is perpendicular to the boundary surface for both members. Thus, the axial force and bending moment in members BC and BH may be written in terms of the member end point displacements as

$$\begin{aligned}
N_{BC} &= \frac{EA}{2L}\left(v_B\cos\theta + w_B\sin\theta\right) \\
N_{BH} &= \frac{EA}{2\sqrt{2}b}\left(u_H + v_H^B\right) \\
M_{BC}(s) &= \left(\frac{3EI}{L^2} - \frac{6EI}{L^3}s\right)\left(-v_B\sin\theta + w_B\cos\theta\right) \\
M_{BH}(s) &= \left(\frac{3\sqrt{2}EI}{2b^2} - \frac{3\sqrt{2}EI}{b^3}s\right)\left(-u_H + v_H^B\right)
\end{aligned} \tag{9}$$

Setting $u_H = -\bar{u}$ and $w_B = -\bar{w}$ and making the substitutions $v_B = \left(\frac{v_B}{\bar{v}}\right)\bar{v}$ and $v_H^B = \left(\frac{v_H^B}{\bar{v}}\right)\bar{v}$ in equation (9), the strain energy in members BC and BH are written in terms of the unit cell boundary displacements using equation (8) as

$$\begin{aligned}
U_{BC} &= \frac{EA}{4L}\left[\left(\frac{v_B}{\bar{v}}\right)\bar{v}\cos\theta - \bar{w}\sin\theta\right]^2 + \frac{3EI}{L^3}\left[-\left(\frac{v_B}{\bar{v}}\right)\bar{v}\sin\theta - \bar{w}\cos\theta\right]^2 \\
U_{BH} &= \frac{EA}{8b}\left[-\bar{u} + \left(\frac{v_H^B}{\bar{v}}\right)\bar{v}\right]^2 + \frac{3EI}{2b^3}\left[\bar{u} + \left(\frac{v_H^B}{\bar{v}}\right)\bar{v}\right]^2
\end{aligned} \tag{10}$$

The work applied to the unit cell by the application of the applied stress σ_{yy} acting over the displacement $\bar{v}$ is

$$W = \left[\sigma_{yy}\left(2L\sin\theta\right)\left(L\cos\theta + \frac{b}{\sqrt{2}}\right)\right]\bar{v} \tag{11}$$

The product of the terms in square brackets in equation (11) represents the total force applied to the unit cell in the Y-direction, a force which is statically equivalent to the applied stress σ_{yy} acting over the area $(2L\sin\theta)\left(L\cos\theta+\frac{b}{\sqrt{2}}\right)$.

Following Zhu, et al. (1997), we next apply the Theorem of Minimum Potential Energy (Love, 1944), which is

$$\frac{\partial U}{\partial \overline{u}}=0 \qquad \frac{\partial U}{\partial \overline{v}}=0 \qquad \frac{\partial U}{\partial \overline{w}}=0$$

Direct substitution of the expression for U from equations (6) and (10), however, leads to a trivial result. Since $W=2U$ and therefore $U=W-U$, we can write a mixed and more useful form of U which includes the applied stress and the unit cell boundary displacements. A more convenient form of the Minimum Potential Energy Theorem is then

$$\frac{\partial(W-U)}{\partial \overline{u}}=0 \qquad \frac{\partial(W-U)}{\partial \overline{v}}=0 \qquad \frac{\partial(W-U)}{\partial \overline{w}}=0 \tag{12}$$

Substituting equation (10) into equation (6) and substituting the result along with equation (11) into equation (12) leads to the following set of three simultaneous equations written in terms of the boundary displacements

$$\left(\frac{12EI}{b^3}+\frac{EA}{b}\right)\overline{u}+\left(\frac{12EI}{b^3}-\frac{EA}{b}\right)\left(\frac{v_H^B}{\overline{v}}\right)\overline{v}=0 \tag{13a}$$

$$\left(\frac{12EI}{b^3}-\frac{EA}{b}\right)\left(\frac{v_H^B}{\overline{v}}\right)\overline{u}+\left[\left(\frac{2EA}{L}\cos^2\theta+\frac{24EI}{L^3}\sin^2\theta\right)\left(\frac{v_B}{\overline{v}}\right)^2+\left(\frac{12EI}{b^3}+\frac{EA}{b}\right)\left(\frac{v_H^B}{\overline{v}}\right)^2\right]\overline{v}$$
$$-\left[\left(\frac{2EA}{L}-\frac{24EI}{L^3}\right)\left(\frac{v_B}{\overline{v}}\right)\cos\theta\sin\theta\right]\overline{w}=2\sigma_{yy}L\sin\theta\left(2L\cos\theta+\sqrt{2}b\right) \tag{13b}$$

$$-\left[\left(\frac{EA}{L}-\frac{12EI}{L^3}\right)\left(\frac{v_B}{\overline{v}}\right)\cos\theta\sin\theta\right]\overline{v}+\left(\frac{12EI}{L^3}\cos^2\theta+\frac{EA}{L}\sin^2\theta\right)\overline{w}=0 \tag{13c}$$

Using equation (7), the solution to equation (13) yields

$$\bar{u} = -\sigma_{yy}\left(L\sin\theta\right)\left(2L\cos\theta+\sqrt{2}b\right)\left\{\frac{b}{2AE}-\frac{b^3}{24EI}\right\} \tag{14a}$$

$$\bar{v} = \sigma_{yy}\left(L\sin\theta\right)\left(2L\cos\theta+\sqrt{2}b\right)\left\{\frac{2L\cos^2\theta+b}{2AE}+\frac{2L^3\sin^2\theta+b^3}{24EI}\right\} \tag{14b}$$

$$\bar{w} = -\sigma_{yy}\left(L\sin\theta\right)\left(2L\cos\theta+\sqrt{2}b\right)\left\{\frac{L}{AE}-\frac{L^3}{12EI}\right\}\cos\theta\sin\theta \tag{14c}$$

Since the Young's modulus in the Y-direction is $E_y = \dfrac{\sigma_{yy}}{\varepsilon_{yy}}$, substituting the expression for $\bar{v}$ from equation (14b) into the expression for ε_{yy} from equation (5) yields

$$E_y = \frac{12EI}{L\sin\theta\left[2L^3\sin^2\theta+b^3+\dfrac{12I}{A}\left(2L\cos^2\theta+b\right)\right]} \tag{15}$$

Furthermore, we have for the Poisson's ratios

$$\upsilon_{yx} = \frac{-\varepsilon_{xx}}{\varepsilon_{yy}} = \frac{\bar{u}}{\bar{v}}$$

and (16)

$$\upsilon_{yz} = \frac{-\varepsilon_{zz}}{\varepsilon_{yy}} = \frac{\bar{w}\left(2L\cos\theta+\sqrt{2}b\right)}{4\bar{v}L\sin\theta}$$

which upon substitution of the expressions for $\bar{v}$ and $\bar{w}$ become

$$\upsilon_{yx} = \frac{b\left(Ab^2-12I\right)}{12I\left(2L\cos^2\theta+b\right)+A\left(2L^3\sin^2\theta+b^3\right)}$$

and (17)

$$\upsilon_{yz} = \frac{\left(AL^2-12I\right)\left(2L\cos\theta+\sqrt{2b}\right)\cos\theta}{2\left[12I\left(2L\cos^2\theta+b\right)+A\left(2L^3\sin^2\theta+b^3\right)\right]}.$$

The axial force and maximum moment in the members of length L (members BC and FG) are obtained by substituting the expressions for v_B and w_B into the expressions for N_{BC} and M_{BC} in equation (9). The maximum moment occurs at the member ends, at either $s = 0$ or $s = L$. Recalling that $-w_B = \overline{w}$, the expression for v_B and w_B are obtained from the first expression in equation (7) and from equation (14). Substituting these into equation (9) yields

$$M_{BC} = M_{FG} = \frac{\sigma_{yy}}{2}(L\sin\theta)^2\left(2L\cos\theta + \sqrt{2}b\right)$$
$$N_{BC} = N_{FG} = \sigma_{yy}\left(2L\cos\theta + \sqrt{2}b\right)L\cos\theta\sin\theta \tag{18}$$

The maximum stress in any member is $\sigma_{\max} = \frac{N}{A} + \frac{M}{S}$, where S is the foam edge section modulus. Substituting equation (18) leads to

$$\sigma_{yy} = \frac{\sigma_{\max}}{\left[\frac{L\cos\theta\sin\theta}{A} + \frac{L^2\sin^2\theta}{2S_x^L}\right]\left[2L\cos\theta + \sqrt{2}b\right]} \tag{19}$$

where S_x^L is the section modulus for the members of length L bending about the section neutral axis which is parallel to the unit cell X-direction.

We assume that foam failure occurs when the foam stresses produce a maximum stress in any of the edges which is equal to the ultimate strength of the solid material, that is when $\sigma_{\max} = \sigma^{ult}$. We will assume that this criterion holds true whether the maximum stress is tensile or compressive. Therefore, the ultimate strength of the foam in the Y-direction, based on failure of the edges of length L, is given as

$$\sigma_{yy}^{ult} = \frac{\sigma^{ult}}{\left[\frac{L\cos\theta\sin\theta}{A} + \frac{L^2\sin^2\theta}{2S_x^L}\right]\left[2L\cos\theta + \sqrt{2}b\right]} \tag{20}$$

The maximum moment and axial force in the members BH and DF is

$$M_{BH} = M_{DF} = \frac{\sigma_{yy}}{2\sqrt{2}}Lb\sin\theta\left(2L\cos\theta + \sqrt{2}b\right)$$
$$N_{BH} = N_{DF} = \frac{\sigma_{yy}}{\sqrt{2}}L\sin\theta\left(2L\cos\theta + \sqrt{2}b\right) \tag{21}$$

This leads to

$$\sigma_{yy} = \frac{\sigma_{max}}{\left[\frac{L\sin\theta}{\sqrt{2}A} + \frac{Lb\sin\theta}{2\sqrt{2}S_z^b}\right]\left[2L\cos\theta + \sqrt{2}b\right]} \tag{22}$$

where S_z^b is the section modulus for members of length b bending about the section neutral axis which is parallel to the unit cell Z-direction. The ultimate foam strength, based on failure of these members of length b, is therefore

$$\sigma_{yy}^{ult} = \frac{\sigma^{ult}}{\left[\frac{L\sin\theta}{\sqrt{2}A} + \frac{Lb\sin\theta}{2\sqrt{2}S_z^b}\right]\left[2L\cos\theta + \sqrt{2}b\right]} \tag{23}$$

In low density foams, bending stresses tend to be much more significant in contributing to material failure than the axial force contributions (Huber and Gibson (1988) and Ridha, et al. (2006)). Ignoring the axial terms in equations (20) and (23), the denominator in equation (20) will always be larger than the denominator in equation (23) as long as the unit cell is elongated such that $\sqrt{2}\sin\theta > \frac{S_x^L b}{S_z^b L}$. As a result, the edges with length L will fail at a lower applied stress σ_{yy} than the edges with length b and hence equation (20) will always yield a lower estimate of the ultimate strength than equation (23).

2.4 Loading in the Z-direction (Rise)

We now seek to develop an analogous set of equations for loading in the Z (rise) direction. For loading in the Z-direction, it is more convenient to use the repeating unit shown in figure 4. Since the members *AC*, *BC*, *DC*, and *CE* lie within the boundaries of the unit cell, and are not shared by an adjacent unit cell, it will be assumed that they have area *A* and moment of inertia *I*.

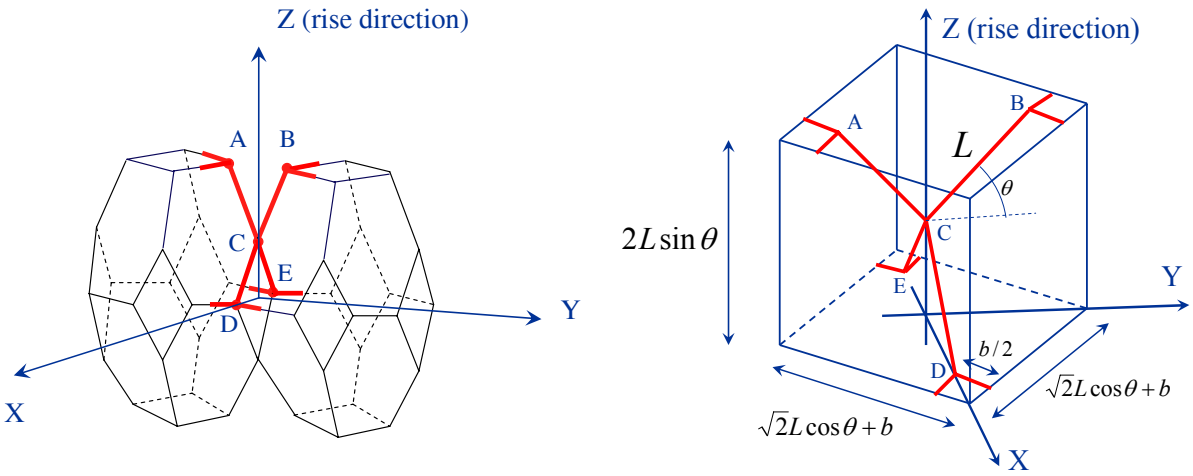

Figure 4.—Repeating unit cell for loading in the Z-direction (rise direction).

We define the unit cell displacements relative to point *C*, so that $u_C = v_C = w_C = 0$ and impose the conditions on the displacements:

$$\begin{aligned} u_D &= -u_E = -\bar{u} \\ v_A &= -v_B = \bar{v} \\ w_A &= w_B = \bar{w} \\ w_D &= w_E = -\bar{w} \end{aligned} \tag{24}$$

Again, the deformation of the unit cell is assumed to occur with no rotation of the member end points.

The displaced shape is illustrated in figure 5. Due to the anti-symmetry of the unit cell, $\bar{u} = \bar{v}$ and therefore $\varepsilon_{xx} = \varepsilon_{yy}$. The relations between the unit cell strains and the boundary displacements are

$$\varepsilon_{xx} = \varepsilon_{yy} = \frac{-2\bar{v}}{2L\cos\theta + \sqrt{2}b} \qquad \varepsilon_{zz} = \frac{\bar{w}}{L\sin\theta} \tag{25}$$

The members of length *b* are unstressed and therefore do not contribute to the total strain energy of deformation. Also, since the four members of length *L* all have the same end displacements, they have the same axial force and bending moments. The total strain energy of deformation for the unit cell is therefore four times the strain energy of any of one these members, that is $U = 4U_{AC} = 4U_{BC} = 4U_{CD} = \ldots$

The axial force and bending moment in member *BC* is

$$\begin{aligned} N_{BC} &= \frac{EA}{L}\left(v_B\cos\theta + w_B\sin\theta\right) \\ M_{BC}(s) &= \left(\frac{6EI}{L^2} - \frac{12EI}{L^3}s\right)\left(-v_B\sin\theta + w_B\cos\theta\right) \end{aligned} \tag{26}$$

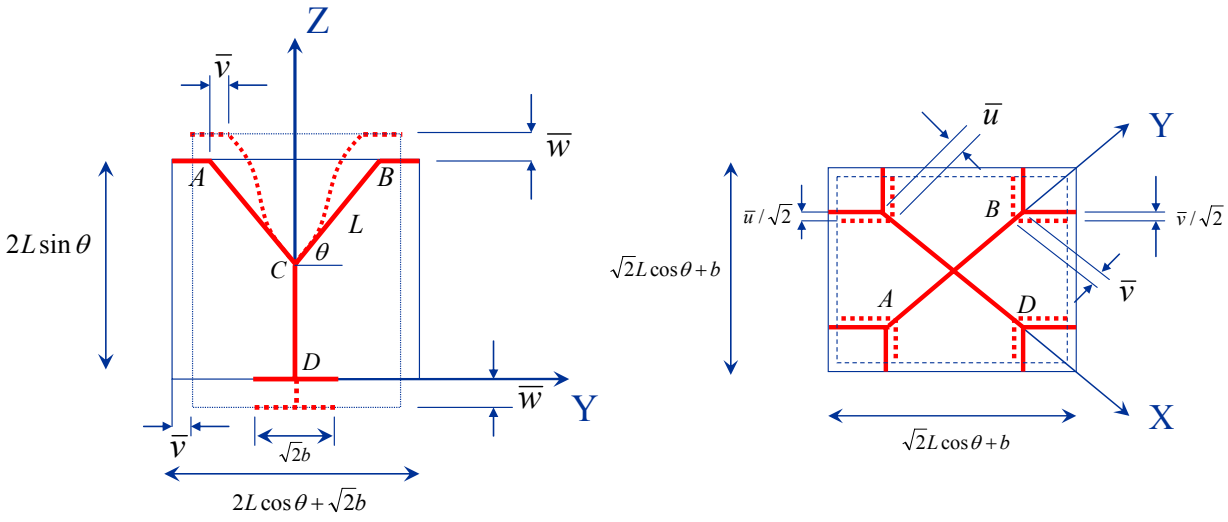

(a) Y-Z plane (b) X-Y plane

Figure 5.—Unit cell deformation for loading in the Z-direction.

Making the substitutions $v_B = -\bar{v}$ and $w_B = \bar{w}$ in equation (26) and using equation (8), the strain energy of deformation is obtained as

$$U = 4U_{BC} = \frac{2EA}{L}\left(-\bar{v}\cos\theta + \bar{w}\sin\theta\right)^2 + \frac{24EI}{L^3}\left(\bar{v}\sin\theta + \bar{w}\cos\theta\right)^2 \tag{27}$$

The work performed by the applied stress σ_{zz} acting over the displacement $\bar{w}$ on the top face and over the displacement $-\bar{w}$ on the bottom face is

$$W = 2\sigma_{zz}\left(\sqrt{2}L\cos\theta + b\right)^2 \bar{w} \tag{28}$$

Applying the Minimum Potential Energy Theorem yields the set of equations

$$\left(A\cos^2\theta + \frac{12I}{L^2}\sin^2\theta\right)\bar{v} - \left(A - \frac{12I}{L^2}\right)\cos\theta\sin\theta\,\bar{w} = 0 \tag{29a}$$

$$-\left(\frac{2EA}{L} - \frac{24EI}{L^3}\right)\cos\theta\sin\theta\,\bar{v} + \left(\frac{24EI}{L^3}\cos^2\theta + \frac{2EA}{L}\sin^2\theta\right)\bar{w} = \sigma_{zz}\left(\sqrt{2}L\cos\theta + b\right)^2 \tag{29b}$$

the solution to which yields

$$\bar{v} = -\sigma_{zz}\left(\sqrt{2}L\cos\theta + b\right)^2\left\{\frac{L}{2AE} - \frac{L^3}{24EI}\right\}\cos\theta\sin\theta \tag{30a}$$

$$\bar{w} = \sigma_{zz}\left(\sqrt{2}L\cos\theta + b\right)^2\left\{\frac{L\sin^2\theta}{2AE} + \frac{L^3\cos^2\theta}{24EI}\right\} \tag{30b}$$

The Young's modulus $E_z = \left(\frac{\sigma_{zz}}{\varepsilon_{zz}}\right)$ is obtained by substituting the expression for $\bar{w}$ from equation (30b) into equation (25), which results in

$$E_z = \frac{24EI\sin\theta}{L^2\left[\cos^2\theta + \frac{12I\sin^2\theta}{AL^2}\right]\left[\sqrt{2}L\cos\theta + b\right]^2} \tag{31}$$

Since $\varepsilon_{xx} = \varepsilon_{yy}$, then $\upsilon_{zx} = \upsilon_{zy}$. Using $\upsilon_{zx} = \upsilon_{zy} = -\frac{\varepsilon_{yy}}{\varepsilon_{zz}}$, we get

$$\upsilon_{zx} = \upsilon_{zy} = \frac{-\varepsilon_{yy}}{\varepsilon_{zz}} = \frac{2\bar{v}L\sin\theta}{\bar{w}\left(2L\cos\theta + \sqrt{2}b\right)} \tag{32}$$

and upon substituting the expressions for the displacements from equation (30), equation (32) becomes

$$\upsilon_{zx} = \upsilon_{zy} = \frac{\sqrt{2}L^2\left(AL^2 - 12I\right)\cos\theta\sin^2\theta}{\left[12IL\sin^2\theta + AL^3\cos^2\theta\right]\left[\sqrt{2}L\cos\theta + b\right]} \tag{33}$$

Substituting the expressions from equation (30) into equation (26) yields for the axial force and maximum bending moment

$$N_{BC} = \frac{\sigma_{zz}\sin\theta}{2}\left(\sqrt{2}L\cos\theta + b\right)^2$$

$$M_{BC} = \frac{\sigma_{zz}\,L\cos\theta}{4}\left(\sqrt{2}L\cos\theta + b\right)^2 \tag{34}$$

Since $\sigma_{\max} = \frac{N}{A} + \frac{M}{S}$, we obtain

$$\sigma_{zz} = \frac{\sigma_{\max}}{\left[\frac{\sin\theta}{2A} + \frac{L\cos\theta}{4S_x^L}\right]\left[\sqrt{2}L\cos\theta + b\right]^2} \tag{35}$$

and therefore the ultimate strength of the foam in the Z-direction is given as

$$\sigma_{zz}^{ult} = \frac{\sigma^{ult}}{\left[\frac{\sin\theta}{2A} + \frac{L\cos\theta}{4S_x^L}\right]\left[\sqrt{2}L\cos\theta + b\right]^2} \tag{36}$$

2.5 Stiffness and Strength Ratios

Defining the stiffness ratio as $R_E = \frac{E_z}{E_y}$, then equations (1), (2), (15), and (31) lead to

$$R_E = \frac{R^2}{4}\frac{\left[2\sin^2\theta + \left(\frac{b}{L}\right)^3 + \frac{12I}{AL^2}\left(2\cos^2\theta + \frac{b}{L}\right)\right]}{\left[\cos^2\theta + \frac{12I}{AL^2}\sin^2\theta\right]} \tag{37}$$

Defining the strength ratio as $R_\sigma = \frac{\sigma_{zz}^{ult}}{\sigma_{yy}^{ult}}$ and assuming that foam failure in the Y-direction occurs due to failure of the members of length *L*, then equations (1), (2), (19), and (35) lead to

$$R_\sigma = R\frac{2S_x^L\cos\theta + AL\sin\theta}{2S_x^L\sin\theta + AL\cos\theta} \tag{38}$$

2.6 Isotropic Foams

In the special case of isotropic foams with an equi-axed repeating unit, we have the conditions $H = D$ and $E_y = E_z$, or in terms of the aspect and stiffness ratios, $R = R_E = 1$. Using equation (37), it is easily shown that these two conditions are only satisfied when $b = L$ and $\theta = \frac{\pi}{4}$. Setting $b = L$ and $\theta = \frac{\pi}{4}$, both equations (15) and (31) reduce to

$$E_y = E_z = \frac{6\sqrt{2}EI}{L^4\left[1+\frac{12I}{AL^2}\right]} = E^* \tag{39}$$

which is the expression obtained by Zhu, et al. (1997) for isotropic, open-celled foams. Also, the expressions for the Poisson's ratios, equations (17) and (33), all reduce to

$$\upsilon^* = 0.5\frac{\left(AL^2 - 12I\right)}{\left(AL^2 + 12I\right)}$$

the expression for the Poisson's ratio obtained by Zhu, et al. (1997) for the isotropic case. Furthermore, the relative density becomes $\gamma = \frac{3A}{2\sqrt{2}\,L^2}$.

3. Application to Experimental Studies

3.1 Relative Modulus Versus Relative Density in Isotropic Foams

We first apply the equations derived in the previous section to simulate the variation of the relative modulus $\frac{E^*}{E}$ with the relative density γ for isotropic foams. For isotropic foams, the relative modulus follows from equation (39). Assuming that the edge cross-sections are circular with radius r, the relative modulus is

$$\frac{E^*}{E} = \frac{6\sqrt{2}\pi}{4}\frac{\left(\frac{r}{L}\right)^4}{1+3\left(\frac{r}{L}\right)^2} \tag{40}$$

and the relative density is

$$\gamma = \frac{3\pi\left(\frac{r}{L}\right)^2}{2\sqrt{2}} \tag{41}$$

Solving equation (41) for the ratio $\frac{r}{L}$ and substituting the result into equation (40) leads to

$$\frac{E^*}{E} = \frac{4\sqrt{2}}{3}\frac{\gamma^2}{\pi + 2\sqrt{2}\,\gamma} \tag{42}$$

By comparison, the relative modulus for a square cross-section is $\frac{4\sqrt{2}\,\gamma^2}{3\left(3+2\sqrt{2}\,\gamma\right)}$, which is similar to equation (42), except that π is replaced by 3.

The variation of the relative modulus with the relative density given by equation (42) is plotted in figure 6 along with the experimental measurements reported by a number of previous researchers. The results are plotted on a log-log scale. Equation (42) provides a good correlation with the experimental results, particularly at low relative densities.

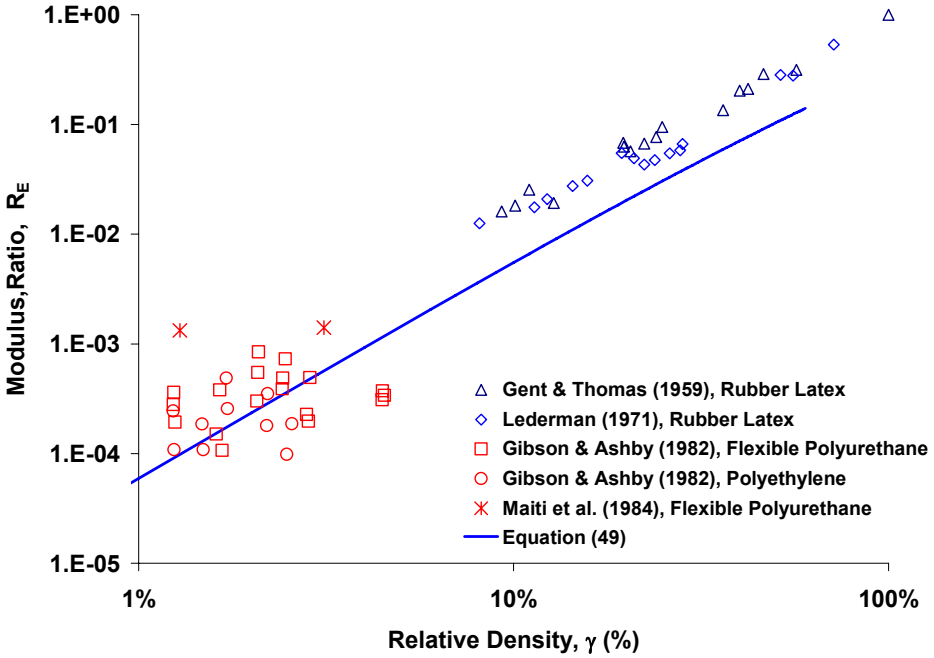

Figure 6.—Relative modulus plotted versus relative density for isotropic, open-celled foam. Results from previous experimental studies are plotted along with the relation given by equation (42).

3.2 Stiffness and Strength Ratio Versus Cell Aspect Ratio and Relative Density for Non-isotropic Foams With a Restricted Unit Cell Geometry

The stiffness ratio and its dependence on the cell aspect ratio has been measured and reported by previous researchers for several non-isotropic polymer foams and the variation of the strength ratio with cell aspect ratio for Porolon was measured by Polyakov and Tarakanov (1967). In this section, we seek to rewrite the equations derived in section 2 for the ratios R_E and R_σ, and obtain expressions for these ratios in terms of the two variables R and γ, so that we may compare the model predictions with the measurements made by previous researchers.

In view of equations (37), (38), and (2), it is clear that the modulus ratio R_E and the strength ratio R_σ are functions of θ, b, L and the cross-section properties. In order to rewrite the expressions for R_E and R_σ in terms of R and γ, it is necessary to impose an additional condition on the unit cell geometry to reduce the number of unknown micro-structural dimensions by one. We impose the condition on the elongated Kelvin model that $\frac{b}{L} = \sqrt{2}\cos\theta$, which was originally suggested by Dement'ev and Tarakanov (1970) and also assumed by Gong, et al. (2005a). This constraint leads to $D = 4L\cos\theta$ and $R = \tan\theta$ and thus

$$\cos\theta = \frac{1}{\sqrt{1+R^2}} \qquad \sin\theta = \frac{R}{\sqrt{1+R^2}} \qquad \frac{b}{L} = \frac{\sqrt{2}}{\sqrt{1+R^2}} \tag{43}$$

Furthermore, the relative density, equation (3), now becomes

$$\gamma = \frac{A}{8L^2}\frac{\left[2\left(1+R^2\right)^{3/2} + \sqrt{2}\left(1+R^2\right)\right]}{R} \tag{44}$$

Substituting the relations in equation (43) into equations (37) and (38) yields

$$R_E = \frac{R^2}{4}\frac{\left[2R^2 + \frac{2\sqrt{2}}{\sqrt{1+R^2}} + \frac{12I}{AL^2}\left(2+\sqrt{2}\sqrt{1+R^2}\right)\right]}{1+\frac{12I}{AL^2}R^2} \tag{45}$$

and

$$R_\sigma = R\frac{\left(\frac{2S_x^L}{AL}\right)+R}{\left(\frac{2S_x^L}{AL}\right)R+1} \tag{46}$$

If we again assume that the edge cross-section is circular with a radius r, then $\frac{12I}{AL^2} = 3\left(\frac{r}{L}\right)^2$ and $\frac{2S_x^L}{AL} = \frac{r}{2L}$, and equation (44) may be rearranged to obtain

$$\frac{12I}{AL^2} = 3\left(\frac{r}{L}\right)^2 = \frac{24R\gamma}{2\pi\left(1+R^2\right)^{3/2} + \sqrt{2}\,\pi\left(1+R^2\right)}$$

and (47)

$$\frac{2S_x^L}{AL} = \frac{r}{2L} = \frac{\sqrt{2R\gamma}}{\sqrt{2\pi\left(1+R^2\right)^{3/2} + \sqrt{2}\,\pi\left(1+R^2\right)}}$$

Substituting the relations in equation (47) into equations (45) and (46) leads to

$$R_E = R^2 \frac{\left[\left(R^2 + \frac{\sqrt{2}}{\sqrt{1+R^2}}\right)\pi + \frac{12\left(2+\sqrt{2\left(1+R^2\right)}\right)R}{\left(1+R^2\right)\left(\sqrt{2}+2\sqrt{1+R^2}\right)}\gamma\right]}{2\left[\pi + \frac{24R^3}{\left(1+R^2\right)\left(\sqrt{2}+2\sqrt{1+R^2}\right)}\gamma\right]} \tag{48}$$

and

$$R_\sigma = R\frac{\sqrt{2R\gamma} + R\sqrt{2\pi\left(1+R^2\right)^{3/2} + \sqrt{2}\pi\left(1+R^2\right)}}{R\sqrt{2R\gamma} + \sqrt{2\pi\left(1+R^2\right)^{3/2} + \sqrt{2}\pi\left(1+R^2\right)}} \tag{49}$$

We note, once again, that an expression similar to equation (48) is obtained if a square cross-section is assumed, except, in that case, π in the numerator and denominator is replaced by a 3.

Equations (48) and (49) are analogous to equation (1) and (4) in Huber and Gibson (1988). Although considerably more cumbersome, equations (48) and (49) are more inclusive than Huber and Gibson's relations, as they account for both axial and bending deformations of the cell edges and they include the effect of the relative density on the stiffness and strength ratios.

Using equation (48), the modulus ratio is plotted versus cell aspect ratio and relative density in figure 7. The experimental results reported by a number of previous researchers are also included. Note that the stiffness ratio is a weak function of the relative density, particularly as the cell aspect ratio approaches unity. As the cell aspect ratio approaches unity, all the curves must collapse to the same point, that is, at $R = 1$ and $R_E = 1$.

The variation of the strength ratio with the cell aspect ratio, given by equation (49), is plotted in figure 8. The variation of the strength ratio with the cell aspect ratio for Porolon as reported by Dement'ev and Tarakanov (1970) (originally reported by Polyakov and Tarakanov (1967)) is also plotted

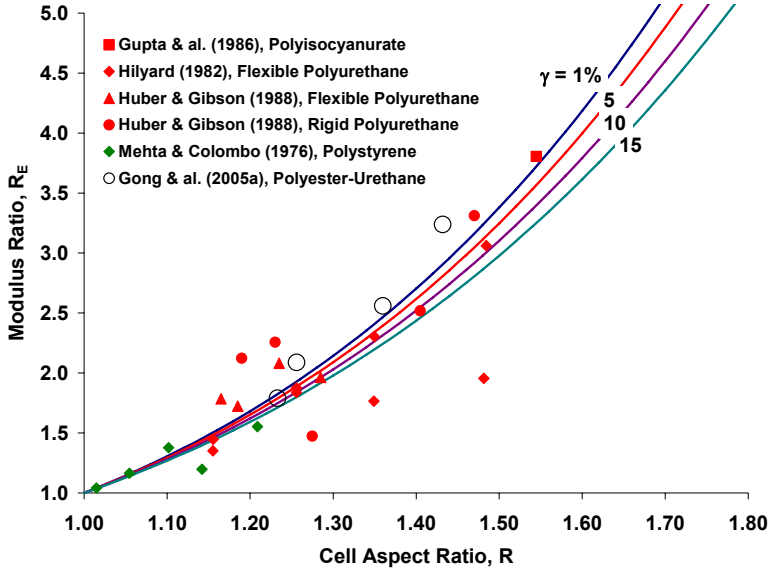

Figure 7.—Modulus ratio plotted versus cell aspect ratio and relative density. Results from previous experimental studies are plotted along with that given by equation (48).

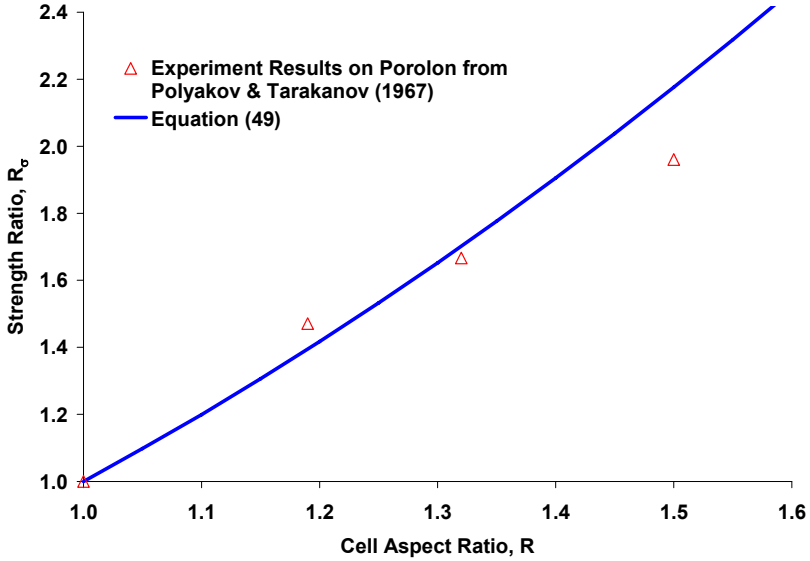

Figure 8.—Strength ratio plotted versus cell aspect ratio. Results on Porolon from Polyakov and Tarakanov (1967) as reported by Dement'ev and Tarakanov (1970) plotted along with equation (49) for γ = 3 percent.

in figure 8. A relative density of 0.03 was used to plot equation (49), as this was the relative density reported in the experimental study. Clearly, equation (49) provides a reasonably-close match with the measured results, given the small amount of the experimental data available.

3.3. Analysis of Polymer Foams Using a General Description of the Unit Cell Geometry

We now apply the equations derived in section 2 to simulate the strength behavior of the rigid polyurethane foams reported by Huber and Gibson (1988). We will allow for the most general description of the unit cell geometry, which requires us to specify three dimensions to describe the unit cell geometry

plus a description of the edge cross-section. We will assume a circular edge cross-section and therefore we need only to define the cross-section radius. Using the values for the cell width, the cell aspect ratio, the relative density and the modulus ratio reported in Huber and Gibson (1988), we use the equations derived in section 2 to calculate the unit cell dimensions and the edge cross-section radius for each of the five rigid polyurethane foams. Using these four dimensions, the strength ratio for each of the five foams can be calculated using a modified form of equation (38).

Now since the rigid polyurethane foams studied in Huber and Gibson (1988) were closed-cell foams, their microstructure includes cell faces which are stressed and deform with the application of the applied stress. As such, the faces also contribute to the foam mechanical behavior. In addition, the edge cross-sections are not really circular, but rather they resemble a three-cusp hypocycloid (Gong, et al. (2005a)). As a result, the edge radii that are calculated for the foams are really an *equivalent* cross-section radius. That is they represent the radius of a circular cross-section possessing a structural rigidity that is equivalent to the combined structural rigidity of the cell faces and the three-cusp hypocycloid edges.

From equation (2), we have

$$\frac{b}{L} = \frac{4\sin\theta - 2R\cos\theta}{\sqrt{2}R} \tag{50}$$

Using $D = \frac{H}{R}$ and equation (1), equation (3) can be written as

$$\gamma = \frac{AR^2\left(2 + \frac{b}{L}\right)}{8L^2\sin^3\theta} \tag{51}$$

Assuming a circular edge cross-section with radius r and upon substituting equation (50), equation (51) can be rewritten and rearranged as

$$\left(\frac{r}{L}\right)^2 = \frac{4\sqrt{2}\gamma\sin^3\theta}{\pi R\left(\sqrt{2}R + 2\sin\theta - R\cos\theta\right)} \tag{52}$$

Also, assuming a circular edge cross-section allows us to replace $\frac{12I}{AL^2}$ with $3\left(\frac{r}{L}\right)^2$ and rewrite equation (37) as

$$\left[6R^2\cos^2\theta - 12R_E\sin^2\theta\right]\left(\frac{r}{L}\right)^2 + 3R^2\left(\frac{b}{L}\right)\left(\frac{r}{L}\right)^2 + R^2\left(\frac{b}{L}\right)^3 + 2R^2\sin^2\theta - 4R_E\cos^2\theta = 0 \tag{53}$$

In order to solve for L, b, θ, and r, we could substitute equations (50) and (52) into equation (53) and, using the identity relation $\cos^2\theta = 1 - \sin^2\theta$, obtain an explicit algebraic equation in $\sin\theta$ which can be solved to obtain the value of θ. The resulting equation is, however, quite cumbersome. Instead, we choose to solve the set of equations (50), (52), and (53) in an iterative manner, whereby these equations are solved in series within each iteration.

The steps in the solution approach were to make an initial guess at the value of the inclination angle θ, substitute this value into (50) and (52) and solve (50) and (52) for $\frac{b}{L}$ and $\frac{r}{L}$, respectively. The values of $\frac{b}{L}$ and $\frac{r}{L}$ were then substituted into equation (53) and equation (53) was solved for θ. This process was repeated until the difference in the value of θ between two successive iterations was within an acceptable tolerance. The standard bisection method (Press, et al., 1992) was implemented to solve equation (53) numerically for θ. The method converged usually within thirty iterations given an initial bracketed guess for the inclination angle between 40 and 75°. Once the final value of θ is obtained from the iterative solution, the value of L is determined from $L = \frac{RD}{4\sin\theta}$ and the value of b and r is calculated from equations (50) and (52), respectively.

The cell width, relative density, cell aspect ratio, modulus ratio and the measured compressive strength ratio for each of the five rigid polyurethane foams reported in Huber and Gibson (1988) are listed in table I. We have also listed the equivalent edge cross-section radius, the inclination angle and the lengths of the edges L and b which were obtained from each iterative solution. Notice that the equivalent cross-section radii seem to correlate with the measured relative densities, and the inclination angles seem to correlate with the measure modulus ratios. Also, although the elongated tetrakaidecahedron shown in figure 1 is drawn so as to imply that the edges of length b are shorter than the edges of length L, this is not strictly true. Indeed, one of the foams listed in table I has $b = L$ and another has $b > L$.

TABLE I.—RESULTS FROM THE EXPERIMENTAL STUDY ON RIGID POLYURETHANE FOAMS BY HUBER AND GIBSON (1988) ALONG WITH THE RESULTS FROM THE NUMERICAL SOLUTION

Experimental data for rigid polyurethane foams from Huber and Gibson (1988)					Solution results				
Cell width, D, mm	Relative density, γ	Cell aspect ratio, R	Modulus ratio, R_E	Exp. comp. strength ratio,[a] R_σ	Edge cross-sectional radius, r, mm	Inclination angle, θ, deg	Edge length, L, mm	Edge length, b, mm	Predicted strength ratio, R_σ
0.20	0.027	1.405	2.518	1.730	0.0070	53.91	0.087	0.069	1.880
0.20	0.053	1.470	3.312	1.943	0.0100	56.63	0.088	0.073	2.132
0.20	0.080	1.230	2.256	1.484	0.0117	53.29	0.077	0.077	1.582
0.20	0.107	1.275	1.475	1.152	0.0137	49.26	0.084	0.064	1.447
0.20	0.133	1.190	2.122	1.455	0.0149	52.98	0.075	0.078	1.498

[a]Experimental compressive strength ratios were calculated from the plastic collapse stresses reported in Huber and Gibson (1988).

Assuming a circular cross-section of radius r, equation (38) becomes

$$R_\sigma = R\frac{\left(\frac{r}{2L}\right)+\tan\theta}{\left(\frac{r}{2L}\right)\tan\theta+1} \tag{54}$$

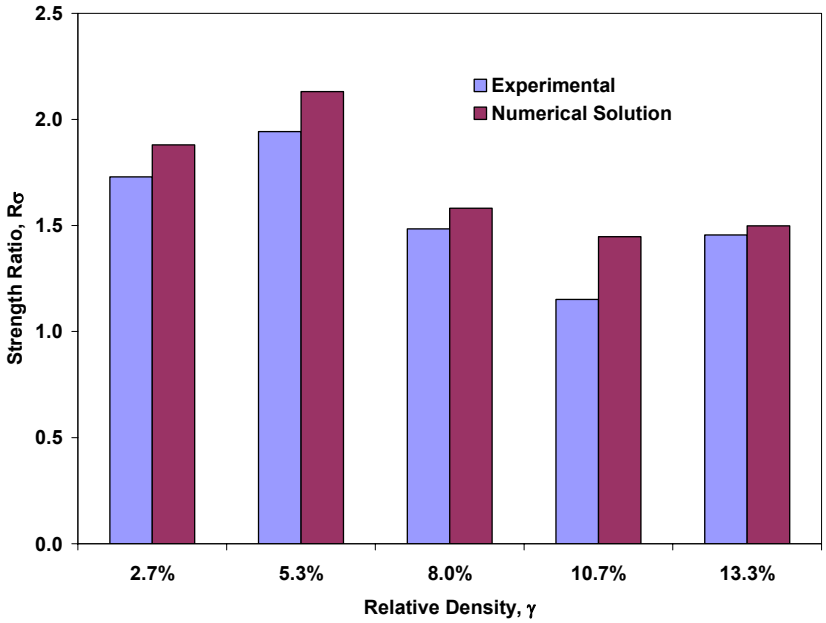

Figure 9.—Comparison of the measured and predicted strength ratio plotted versus the foam relative density for rigid polyurethane foams. Experimental data from Huber and Gibson (1988).

The strength ratio was calculated for each foam using equation (54) and the values of r, θ, and L that were obtained from the iterative solutions along with the measured values of R. The predicted strength ratios are listed in table I; a comparison of the measured and predicted strength ratios is shown in figure 9. The predicted strength ratios are within 10 percent of the measured strength ratios for all cases except for the 10.7 percent relative density foam where the error is close to 26 percent. It should be mentioned that the value of the cell aspect ratio reported by Huber and Gibson (1988), for this foam, was brought into question, as they reported difficulties with the microscope while measuring the micro-structure of this foam. Further, the cell aspect ratio for this foam does not appear to be consistent with the measured strength and stiffness ratios. The measured strength and stiffness ratios for the 10.7 percent relative density foam were the lowest of the five foams, whereas the cell aspect ratio was the median of the five values. Ignoring the results for the 10.7 percent relative density foam, we can conclude that the equations derived in section 2 as well as the iterative solution were successful in predicting the compressive strength ratios for the closed-cell foams studied by Huber and Gibson (1988).

Finally, we note that, for all five cases, the value of the ratio $\frac{b}{L}$ is not equal to the value of $\sqrt{2}\cos\theta$, reinforcing our notion that the restriction on the unit cell geometry used by the previous researchers is unfounded and adopted merely for the sake of convenience.

4. Concluding Remarks

The formulation by Zhu, et al. (1997) has been revised to include the mechanical and strength behavior of non-isotropic foams. Equations for the foam Young's modulus, Poisson's ratio and strength in the principal material directions were obtained by adopting an elongated Kelvin model as the repeating unit cell. These equations were written in terms of the edge lengths and edge cross-section properties, the inclination angle and the strength and stiffness of the solid material. The micro-mechanics model is developed from the most general description of an elongated Kelvin model, as it requires three independent dimensions to describe the unit cell geometry as well as a description of the edge cross-section.

The model was applied to simulate the variation of the relative modulus with relative density in isotropic foams as well as the variation of the modulus ratio and strength ratio with cell aspect ratio in non-isotropic foams. In all cases, the model results were in good agreement with the experimental measurements. The model was also applied to simulate the strength ratio in closed-cell rigid polyurethane foams. Here, also, the model results were in good agreement with the measurements, as the predicted strength ratio was within 10 percent of the measured strength ratios for all but one of the five foams.

In closing, it is worth noting that by adopting an elongated Kelvin model with the most general geometry, a more detailed description of the foam microstructure is required in order to apply the resulting equations and predict the foam behavior. More specifically, it is now necessary to obtain four separate physical and mechanical measurements of the foam in order to apply the equations. Aside from this added burden, the model is an improvement over the previous models, since it is capable of more closely representing the foam micro-structure for a wider range of foam materials. Thus, the resulting equations should more accurately simulate the foam behavior for a wider range of foams.

Appendix
Relation Between the Minimum Allowable Inclination Angle and the Length Ratio *b*/*L* for an Elongated Tetrakaidecahedron

If the height H and width D of the tetrakaidecahedron are equal, the expression in equation (1) leads to

$$2\sin\theta - \cos\theta = \frac{b}{\sqrt{2}L} \tag{A1}$$

For an elongated tetrakaidecahedron ($H > D$), we have the inequality

$$2\sin\theta - \cos\theta > \frac{b}{\sqrt{2}L} \tag{A2}$$

Using the trigonometric identity, $\cos\theta = \sqrt{1-\sin^2\theta}$, equation (A1) can be rearranged and rewritten as a second-order polynomial in sin θ, that is,

$$5\sin^2\theta - 2\sqrt{2}\frac{b}{L}\sin\theta + \left(\frac{b^2}{2L^2} - 1\right) = 0 \tag{A3}$$

The solution to equation (A3) is obtained using the *quadratic formula* resulting in the two solutions

$$\sin\theta_1 = \frac{\sqrt{2}b}{5L} + \frac{\sqrt{2}}{10}\sqrt{10 - \frac{b^2}{L^2}} \tag{A4a}$$

$$\sin\theta_2 = \frac{\sqrt{2}b}{5L} - \frac{\sqrt{2}}{10}\sqrt{10 - \frac{b^2}{L^2}} \tag{A4b}$$

where both roots are real provided $\frac{b}{L} \le \sqrt{10}$ and where the two are identical when $\frac{b}{L} = \sqrt{10}$. The solutions listed in equation (A4) are plotted in figure A1.

It is easily shown that equation (A4a) is the solution to equation (A1) and that equation (A4b) is the solution to

$$2\sin\theta = -\cos\theta + \frac{b}{\sqrt{2}L} \tag{A5}$$

Since equation (A5) has no physical significance here, we will ignore the latter of the two solutions in equation (A4).

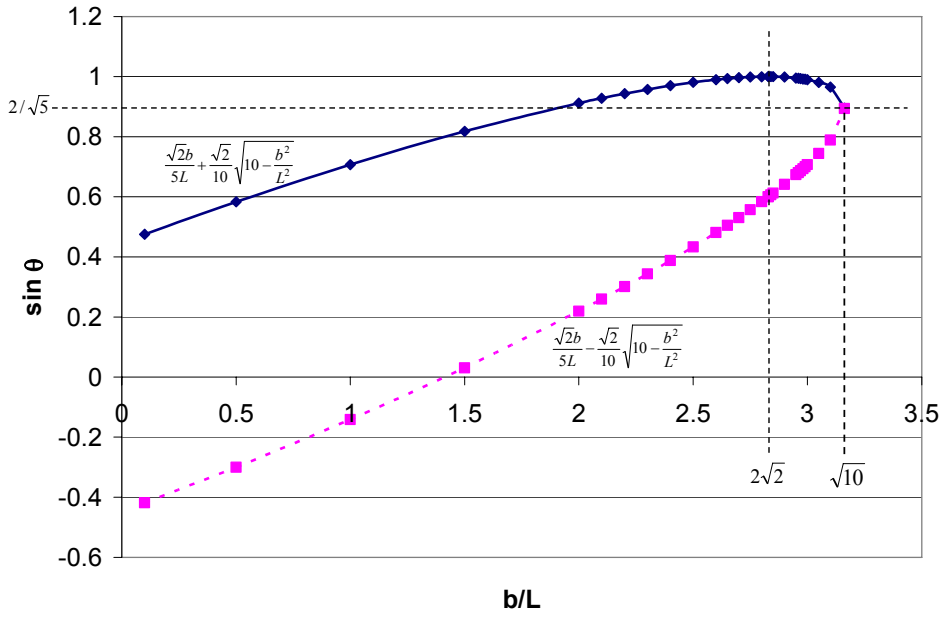

Figure A1.—Plot of the two solutions to equation (A3).

The plot of equation (A4a) in figure A1 defines the value of sin θ as a function of the length ratio $\frac{b}{L}$ for any tetrakaidecahedron with $H = D$. As such, it defines the lower bound on the inclination angle for all possible elongated tetrakaidecahedron, since sin θ for any elongated tetrakaidecahedron must lie above the upper curve in figure A1.

We note that, in the range $\frac{2}{\sqrt{5}} < \sin\theta < 1$, equation (A4a) yields two possible values for the ratio $\frac{b}{L}$ for each value of sin θ. The values of $\frac{b}{L} > 2\sqrt{2}$, however, violate equation (A2) since

$$2 \geq 2\sin\theta - \cos\theta \qquad \text{for all} \qquad \theta \leq \frac{\pi}{2}$$

Hence, for an elongated tetrakaidecahedron with $\theta < \frac{\pi}{2}$, the length ratio $\frac{b}{L}$ must be less than $2\sqrt{2}$.

The lower bound on the inclination angle is therefore given by

$$\theta > Arc\sin\left\{\frac{\sqrt{2}b}{5L} + \frac{\sqrt{2}}{10}\sqrt{10 - \frac{b^2}{L^2}}\right\} \tag{A6}$$

which is valid over the domain $0 < \frac{b}{L} < 2\sqrt{2}$.

References

Chajes, A., 1983. Structural Analysis, Prentice-Hall, Inc., Englewood Cliffs, NJ.

Dement'ev, A.G. and Tarakanov, O.G., 1970. Model analysis of the cellular structure of plastic foams of the polyurethane type. Mekhanika Polimerov **5**, 859–865. Translation Polymer Mechanics **6**, 744–749.

Gent, A.N. and Thomas, A.G., 1959. The deformation of foamed elastic materials. Journal of Applied Polymer Science **I** (1), 107–113.

Gibson, L.J. and Ashby, M.F., 1982. The mechanics of three-dimensional cellular materials. Proc. Roy. Soc. **A382** (1782), 43–59.

Gibson, L.J. and Ashby, M.F., 1997. Cellular Solids: Structure and Properties, Second Edition. Cambridge University Press, Cambridge, UK.

Gong, L., Kyriakides, S., and Jang, W.Y., 2005a. Compressive response of open-celled foams, Part I: Morphology and elastic properties. International Journal of Solids and Structures **42**, 1355–1379.

Gong, L., Kyriakides, S. and Triantafyllidis, N., 2005b. On the stability of Kelvin cell foams under compressive loads. Journal of the Mechanics and Physics of Solids **53**, 771–794.

Gupta, S., Watson, B., Beaumont, P.W.R. and Ashby, M.F., 1986. Final Year Project, Cambridge University Engineering Department, Cambridge, UK.

Hilyard, N.C. (ed.), 1982. Mechanics of Cellular Plastics. Applied Science, London.

Huber, A.T. and Gibson, L.J., 1988. Anisotropy of foams. Journal of Materials Science **23**, 3031–3040.

Laible, J.P., 1985. Structural Analysis. Holt Rinehart and Winston, New York.

Lederman, J.M., 1971. Journal of Applied Polymer Science **15**, 693.

Love, A.E.H., 1944. A Treatise on the Mathematical Theory of Elasticity. Dover Publications, New York, NY.

Maiti, S.K., Gibson, L.J. and Ashby, M.F., 1984. Deformation and energy absorption diagrams for cellular solids. Acta Metal. **32** (11), 1963–1975.

Mehta, B.S. and Colombo, E.A., 1976. Journal of Cellular Plastics **12**, 59.

Polyakov, Y.N. and Tarakanov, O.G., 1967. in: Problems of the Physiochemical Mechanics of Fibrous and Porous Disperse Structures and Materials (in Russian), Riga.

Press W.H., Teukolsky S.A., Vetterling W.T. and Flannery B.P., 1992. Numerical Recipes in FORTRAN: The Art of Scientific Computing, Second Edition. Cambridge University Press, Cambridge, UK.

Ridha, M., Shim,V.P.W. and Yang, L.M., 2006. An elongated tetrakaidecahedral cell model for fracture in rigid polyurethane foam. Key Engineering Materials **306–308**, 43–48.

Thomson, W. (Lord Kelvin), 1887. On the division of space with minimum partitional area. Phil. Mag. **24**, 503–514.

Warren, W.E. and Kraynik, A.M., 1997. Linear elastic behavior of a low-density Kelvin foam with open cells. Journal of Applied Mechanics **64**, 787–794.

Zhu, H.X., Knott, J.F. and Mills, N.J., 1997. Analysis of the elastic properties of open-cell foams with tetrakaidecahedral cells. Journal of the Mechanics and Physics of Solids **45** (3), 319–343.

REPORT DOCUMENTATION PAGE	Form Approved OMB No. 0704-0188

1. REPORT DATE *(DD-MM-YYYY)*	2. REPORT TYPE	3. DATES COVERED *(From - To)*
17-07-2007	Technical Memorandum	

4. TITLE AND SUBTITLE
An Elongated Tetrakaidecahedron Model for Open-Celled Foams

5a. CONTRACT NUMBER

5b. GRANT NUMBER

5c. PROGRAM ELEMENT NUMBER

6. AUTHOR(S)
Sullivan, Roy, M.; Ghosn, Louis, J.; Lerch, Bradley, A.

5d. PROJECT NUMBER

5e. TASK NUMBER

5f. WORK UNIT NUMBER
WBS 524238.08.02.03.04

7. PERFORMING ORGANIZATION NAME(S) AND ADDRESS(ES)
National Aeronautics and Space Administration
John H. Glenn Research Center at Lewis Field
Cleveland, Ohio 44135-3191

8. PERFORMING ORGANIZATION REPORT NUMBER
E-16169

9. SPONSORING/MONITORING AGENCY NAME(S) AND ADDRESS(ES)
National Aeronautics and Space Administration
Washington, DC 20546-0001

10. SPONSORING/MONITORS ACRONYM(S)
NASA

11. SPONSORING/MONITORING REPORT NUMBER
NASA/TM-2007-214931

12. DISTRIBUTION/AVAILABILITY STATEMENT
Unclassified-Unlimited
Subject Categories: 27, 39, and 64
Available electronically at http://gltrs.grc.nasa.gov
This publication is available from the NASA Center for AeroSpace Information, 301-621-0390

13. SUPPLEMENTARY NOTES
Submitted to the International Journal of Solids and Structures.

14. ABSTRACT
A micro-mechanics model for non-isotropic, open-celled foams is developed using an elongated tetrakaidecahedron (Kelvin model) as the repeating unit cell. The micro-mechanics model employs an elongated Kelvin model geometry which is more general than that employed by previous authors. Assuming the cell edges possess axial and bending rigidity, the mechanics of deformation of the elongated tetrakaidecahedron lead to a set of equations for the Young's modulus, Poisson's ratio and strength of the foam in the principal material directions. These equations are written as a function of the cell edge lengths and cross-section properties, the inclination angle and the strength and stiffness of the solid material. The model is applied to predict the strength and stiffness of several polymeric foams. Good agreement is observed between the model results and the experimental measurements.

15. SUBJECT TERMS
Polymeric foam; Non-isotropic; Elongated tetrakaidecahedron (Kelvin) model; Foam material; Elastic material; Energy methods

16. SECURITY CLASSIFICATION OF:			17. LIMITATION OF ABSTRACT	18. NUMBER OF PAGES	19a. NAME OF RESPONSIBLE PERSON
a. REPORT	b. ABSTRACT	c. THIS PAGE			Roy M. Sullivan
U	U	U		31	19b. TELEPHONE NUMBER *(include area code)* 216-433-3249